Structural, electronic and optical properties of the wide band gap semiconductors $KGaQ_2$ (Q = S, Se) and of $AGaTe_2$ (A = K, Cs)

N. Benmekideche

Laboratoire de Caractèisation et Valorisation des Ressources Naturelles, Faculty of SNVSTU, University of Bordj Bou-Arreridj, 34000, Algeria

S. Fetah

Laboratory of Materials and renewable energies, Faculty of science, University of Msila, 28000, Algeria.

Gh. Belgoumri

Laboratoire de Caractèisation et Valorisation des Ressources Naturelles, Faculty of SNVSTU, University of Bordj Bou-Arreridj, 34000, Algeria.

A. Bentabet

Laboratoire de Caractèisation et Valorisation des Ressources Naturelles, Faculty of SNVSTU, University of Bordj Bou-Arreridj, 34000, Algeria.

A. Benmakhlouf

Laboratoire de Caractèisation et Valorisation des Ressources Naturelles, Faculty of SNVSTU, University of Bordj Bou-Arreridj, 34000, Algeria.

Received 28 January 2022; accepted 02 May 2022

In this paper, we studied the structural, electronic and some optical properties of $KGaQ_2$ (Q = S, Se) and $AGaTe_2$ (A = K, Cs) crystals using the pseudopotential plane-wave (PP-PW) method based on density functional theory (DFT), the generalized gradient approximation (GGA) parameterized by Perdew-Burke-Ernzerhof (GGA-PBE) is used for the exchange-correlation (XC) potential. We also use the hybrid density functional (HSE06) to study the electronic structures of these materials. Our results for the equilibrium lattice constants (a, b and c), angle β are in good agreement with experiment data. The electronic structure calculation suggested that crystals are direct-gap semiconductors, employing both the Perdew-Burke-Ernzerhof (PBE) and the hybrid (HSE06) functionals. We note that the hybrid density functional improved the value of band gap, and that the studied compounds are semiconductors with wide band-gaps. We have also predicted the optical properties; the refractive index, the reflection coefficient and dielectric constant on high frequencies.

Keywords: Density functional theory; GGA-PBE; HSE06; $KGaQ_2$ (Q = S, Se); $AGaTe_2$ (A = K, Cs); Structural properties; Electronic properties; Optical constants.

DOI: https://doi.org/10.31349/RevMexFis.68.061003

1. Introduction

The ternary chalcogenide compounds of the ABQ_2 family are known as semiconductors of great interest in the field of electro-optic, and non linear optical applications. During the last decades, these compounds have been extensively studied experimentally because of their industrial interest. Most $ABGa_2$ compounds crystallize in the $KInS_2$ structure C2/c and the ternary potassium compounds, generally, crystallize in the triclinic or in the monoclinic system. Synthesis and XRD characterization of the ternary chalcogenides of aluminum and gallium KMQ_2 (M=Al, Ga and Q = Se, Te) have been performed firstly by Kim and Hughbanks [1]. Later, the single-crystal structures of the ternary gallium selenide $KGaSe_2$, of the potassium gallium sulfide KGaS2 and of the caesium gallium ditelluride $CsGaTe_2$ were synthesized and determined [2-5]. The optical band gaps of $KGaS_2$ and $KGaSe_2$ were experimentally given by Friedrich *et al.*, [6].

In the present work, we explore the theoretical study results of structural and electronic properties of $KGaQ_2$ (Q = S, Se) and of $AGaTe_2$ (A = K, Cs) crystals using first principles calculation. We have also predicted the refractive index, high frequency dielectric constant and reflection coefficient of these materials.

The paper gives a brief description of the computational technique in Sec. 2. Then the results are presented and discussed in Sec. 3. Finally, a conclusion is given in Sec. 4.

2. Computational details

The ab initio calculations were performed using the density functional theory (DFT) based on the pseudo-potential plane wave (PP-PW) method as implemented in the CASTEP code (Cambridge Serial Total Energy Package) [7]. The general-

ized gradient approximation (GGA) applying Perdew-Burke-Ernzerhof (PBE) [8] as exchange-correlation functional was used. Interactions of the valence electrons (K:$3s^2 3p^6 4s^1$, Ga:$3d^{10} 4s^2 4p^1$, Cs:$5s^2 5p^6 6s^1$, S:$3s^2 3p^4$, Se:$4s^2 4p^4$ and Te:$5s^2 5p^4$) with the nucleus and frozen core electrons were treated using the Vanderbilt-type ultra-soft pseudo-potentials [9].

The optimized structural parameters, the lattice constants and the angle β, were determined using the method of structural optimization based on minimization technique of Broyden-Fletcher-Goldfarb-Shanno (BFGS) [10]. After a convergence test, a Monkhorst-Pack mesh [11] of $4 \times 4 \times 2$ for the k points and a plane-wave basis set cutoff of 350 eV were sufficient to ensure a good total energy convergence of 5×10^{-6} eV/atom. The unit-cell was relaxed until the maximum ionic Hellmann-Feynman force was smaller than 0.01 eV/Å^{-1}, within maximum stress of 0.02 GPa and a maximum atomic displacement of 5×10^{-4} Å.

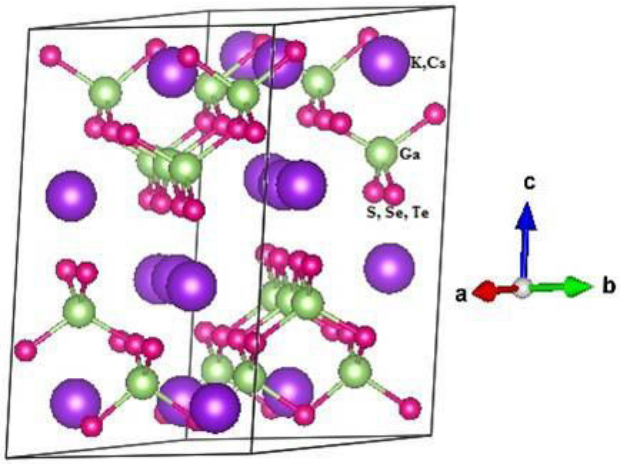

FIGURE 1. Schematic diagram of the monoclinic unit-cell of $AGaQ_2$ (A=K,Cs; Q=S, Se, Te) with 16 formula.

The electronic band structure and associated density of states are calculated with GGA-PBE formalism and moreover the hybrid functional HSE06 was used in order to improves the band gap [12]. The refractive index n, high frequency dielectric constant ϵ, reflection coefficient R for $KGaQ_2$ (Q=S, Se) and $AGaTe_2$ (A=K, Cs) have been calculated using three different models. Ravindra [13], Moss [14] and Herve and Vandamme [5]. These models are related directly with energy gap in semiconductors.

3. Results and discussion

3.1. Structural properties

Single crystal X-ray diffraction analysis revealed that the ternary compounds $AGaQ_2$ (A=K, Cs; Q=S, Se, Te) [1,2,4,5] crystallize in space group C2/c (No. 15) of the monoclinic system and adopt the $TiGaSe_2$ structure type with sixteen formula units per unit-cell (Z=16) as illustrated in Fig. 1. The studied compounds have a layered structure with fundamental building blocks of [Ga4Q10] supertetrahedra. These supertetrahedra form two dimensional (2D) $[GaQ_2]^-$ anionic layers which are separated by K^+ or Cs^+ cations. The conventional cell of $AGaQ_2$(A=K, Cs; Q=S, Se, Te) contains 9 atoms, 2K, 2A and 5Q, the atomic positions and the structural data are given in Tables I, II.

By fully geometry optimization, the calculated equilibrium structural parameters of the studied compounds are summarized in Table I and compared with the available experimental data [1,2,4,5]. The results show that the lattice parameters (a,b,c), angle β, and unit cell equilibrium volume V are in good agreement with the experimental values; the maximum relative error of the calculated equilibrium lattice constants a, b, and c is about 0.24% (2.14%), 0.16% (1.99%) and 0.9% (2.29%) for $KGaS_2$ ($KGaSe_2$), respectively, and, about 1.82% (2.77%), 1.72% (2.46%) and 2.09% (2.52%) for $KGaTe_2$ ($CsGaTe_2$) respectively compared with the respec-

TABLE I. Calculated structural parameters of $KGaQ_2$ (Q = S, Se) and $AGaTe_2$ (A = K, Cs): lattice parameters a (Å), b (Å) and c (Å), angle β (degree) and unit-cell volume V (Å^3).

System		a	b	c		V
$KGaS_2$		10.602	10.594	14.888	100.358	1644.893
	Exp [4]	10.577	10.573	15.023	100.151	1653.771
$KGaSe_2$		11.110	11.089	15.732	99.755	1910.268
	Exp [2]	10.878(2)	10.872(2)	15.380(3)	100.183	1790.360
$KGaTe_2$		11.982	11.978	16.848	100.348	2378.632
	Exp [1]	11.768(3)	11.775(3)	16.503(4)	100.362	2249.590
$CsGaTe_2$		12.137	12.101	18.311	99.507	2652.416
	Exp [5]	11.811	11.811	17.862	99.443	2457.300

TABLE II. Calculated (Cal) and experimental (Exp) atomic positions (x,y,z) for $KGaQ_2$ (Q=S, Se) and $AGaTe_2$(A=K, Cs).

Atoms	wyck	x		y		z	
$KGaS_2$		**Cal**	**Exp [4]**	**Cal**	**Exp [4]**	**Cal**	**Exp [4]**
K1	8f	0.284417	0.284717	0.061594	0.061751	0.388629	0.388988
K2	8f	0.463521	0.463088	0.311280	0.311380	0.110287	0.108864
Ga1	8f	0.145129	0.146065	0.435635	0.436391	0.337673	0.336724
Ga2	8f	0.101458	0.100663	0.188576	0.188546	0.163054	0.163673
S1	8f	0.254787	0.256221	0.311824	0.311729	0.250901	0.250554
S2	8f	0.206513	0.204484	0.064338	0.063389	0.070574	0.072284
S3	8f	0.046135	0.046462	0.311368	0.311495	0.432816	0.431304
S4	4e	0.0	0.0	0.566959	0.568034	0.25	0.25
S5	4e	0.0	0.0	0.056140	0.056786	0.25	0.25
$KGaSe_2$		**Cal**	**Exp [2]**	**Cal**	**Exp [2]**	**Cal**	**Exp [2]**
K1	8f	0.286104	0.28401(17)	0.063250	0.06195(17)	0.385628	0.38710(13)
K2	8f	0.466100	0.46453(19)	0.317229	0.31320(19)	0.107169	0.10870(14)
Ga1	8f	0.142314	0.14545(8)	0.436018	0.43601(8)	0.335555	0.33748(6)
Ga2	8f	0.105524	0.10178(8)	0.188131	0.18898(8)	0.164567	0.16239(6)
Se1	8f	0.258906	0.25913(7)	0.314497	0.31229(9)	0.249931	0.25004(5)
Se 2	8f	0.203527	0.20432(8)	0.055918	0.06225(9)	0.070142	0.06747(6)
Se 3	8f	0.037505	0.04626(9)	0.315025	0.31289(9)	0.430581	0.43495(6)
Se 4	4e	0.0	0.0	0.573591	0.57185(11)	0.25	0.25
Se 5	4e	0.0	0.0	0.055585	0.05366(12)	0.25	0.25
$KGaTe_2$		**Cal**	**Exp [1]**	**Cal**	**Exp [1]**	**Cal**	**Exp [1]**
K1	8f	0.465598	0.464(1)	0.314827	0.316(2)	0.107110	0.1092(9)
K2	8f	0.283600	0.284(1)	0.060953	0.060(2)	0.380425	0.386(1)
Ga1	8f	0.601638	0.6026(5)	0.688237	0.6879(6)	0.162532	0.1620(4)
Ga2	8f	0.145501	0.1462(5)	0.435755	0.4372(6)	0.336585	0.3373(4)
Te1	8f	0.045791	0.0457(4)	0.314243	0.3127(4)	0.436355	0.4354(3)
Te2	8f	0.200804	0.2034(4)	0.058205	0.0624(4)	0.066627	0.0649(2)
Te3	8f	0.262214	0.242(5)	0.311769	0.3128(3)	0.24982	0.248(3)
Te4	4e	0.0	0.0	0.575003	0.566(2)	0.25	0.25
Te5	4e	0.0	0.0	0.050338	0.059(1)	0.25	0.25
$CsGaTe_2$		**Cal**	**Exp [5]**	**Cal**	**Exp [5]**	**Cal**	**Exp [5]**
Cs1	8f	0.285414	0.2871(4)	0.062498	0.0629(4)	0.391777	0.3961(3)
Cs2	8f	0.462188	0.4628(4)	0.312741	0.3123(4)	0.098804	0.1000(3)
Ga1	8f	0.104673	0.1051(5)	0.188083	0.1874(5)	0.171692	0.1709(4)
Ga2	8f	0.143286	0.1442(5)	0.436663	0.4377(5)	0.328145	0.3291(4)
Te 1	8f	0.041814	0.0426(4)	0.312735	0.3124(4)	0.419201	0.4186(3)
Te 2	8f	0.208461	0.2081(4)	0.062351	0.0626(4)	0.081616	0.0803(3)
Te 3	8f	0.261434	0.2600(3)	0.312365	0.3119(5)	0.250110	0.2501(2)
Te 4	4e	0.0	0.0	0.574692	0.5734(5)	0.25	0.25
Te 5	4e	0.0	0.0	0.050311	0.0528(6)	0.25	0.25

tive reported data. There is a slight overestimation of the calculated lattice constants relative to the experimental values. This is not surprising, it is due to the use of the GGA-PBE approximation. The relative deviation of the calculated angle β and unit cell equilibrium volume V deviate by 0.21% (0.42%) and 0.54% (6.7%) for $KGaS_2$ ($KGaSe_2$), and by 0.01% (0.07%) and 5.74% (7.94%) for $KGaTe_2$ ($CsGaTe_2$), respectively, are compared with the experimental data.

It can be seen that the unit cell volume increases from $KGaS_2$, $KGaSe_2$ to $KGaTe_2$, which is assigned to the increasing of the atomic radius from S, Se to Te respectively.

TABLE III. Calculated band gaps energy (E_g) in eV for $KGaQ_2$ (Q=S, Se) and $AGaTe_2$ (A=K, Cs) compared with some experimental and theoretical values.

System	This work PBE	This work HSE06	Experimental	Other calculation
$KGaS_2$	2.588	3.321	–	–
$KGaSe_2$	1.781	2.604	2.60 [2]	1.77 [5]
$KGaTe_2$	1.227	1.777	–	–
$CsGaTe_2$	1.280	1.979	–	–

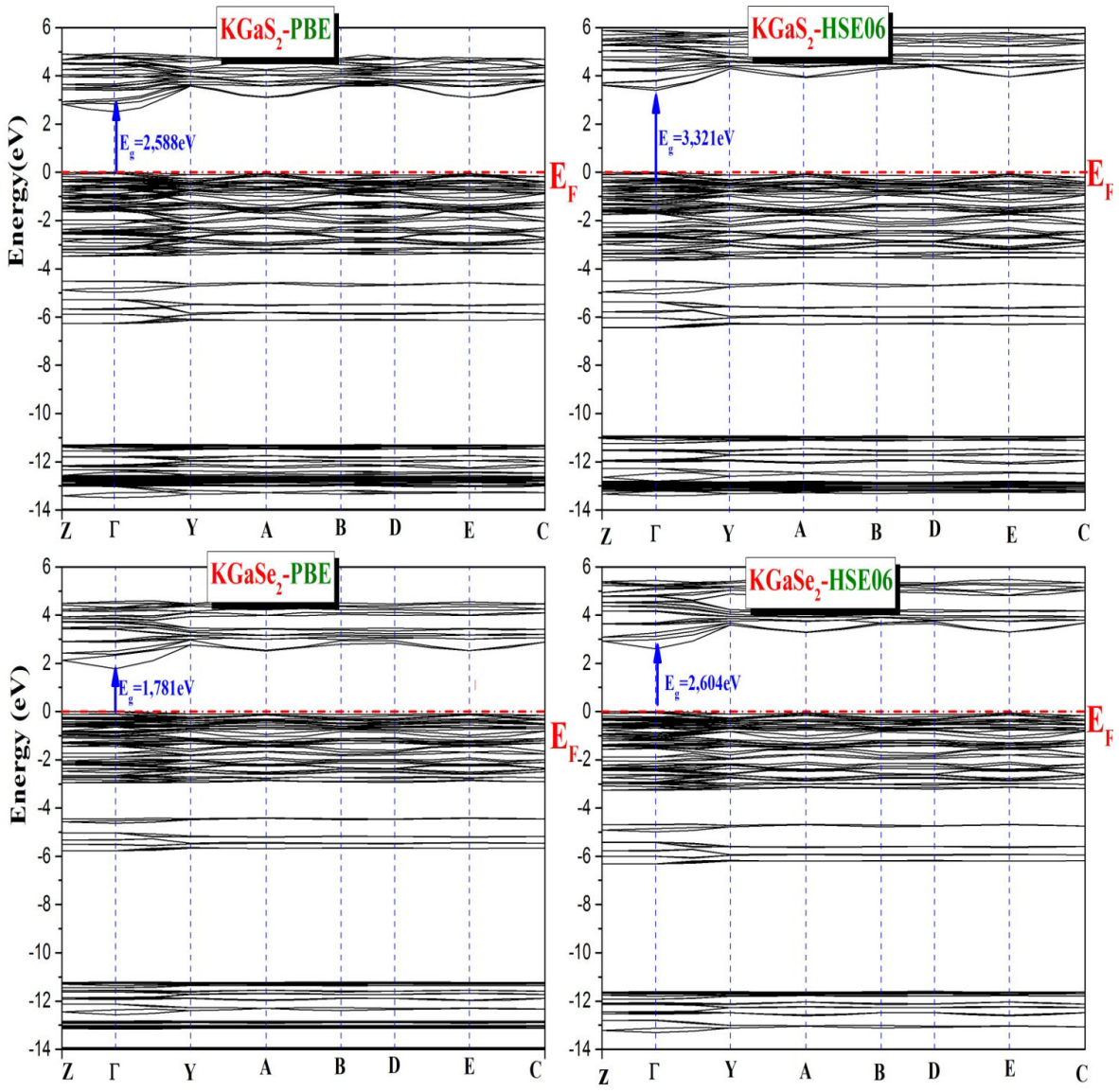

FIGURE 2. Band structure of $KGaQ_2$ (Q=S, Se) calculated along high symmetry lines.

Also, $CsGaTe_2$ unit cell volume is larger than that of $KGaTe_2$, which is also assigned to the small atomic radius of K compared to that of Cs. The calculated atomic positions, listed in Table II, agree well with the experimental data.

3.2. Electronic properties

It is known that GGA-PBE overestimates the band gap of low band gap materials and underestimates the one of high band gap materials [16]. Nevertheless, GGA functionals are known to underestimate Kohn-Sham band gaps (compared to experimentally determined values), whereas the Hartree-Fock (HF) method overestimates them [17]. Therefore, hybrid functionals were introduced by Becke [18] which describe exchange using a combination of the exact nonlocal Hartree-Fock-exchange interaction with GGA. But the computational evaluation became difficult due of the slowly decaying Fock exchange with distance [19]. Heyd *et al.*, suggested an hybrid-functional scheme for extended systems [19,20], giving rise to the Heyd-Scuseria-Ernzerhof (HSE) functional by substituting the exchange energy in the conventional GGA-PBE functional [8] by a functional which mixes HF exchange energy and PBE, the spatial decay of the HF exchange interaction is accelerated by substitution of the full $1/r$ Coulomb potential with a screened one, the exchange energy term is split into short-range (SR) and long-range (LR) components and the long-range exchange energy is given only by the PBE term, and the correlation energy comes entirely from PBE.

$$E_{xc}^{\text{HSE06}} = \frac{1}{4}E_x^{\text{HF,SR}}(w) + \frac{3}{4}E_x^{\text{PBE,SR}}(w) + E_x^{\text{PBE,LR}}(w), \quad (1)$$

where w is the parameter which determines the screening, defining the range of the Hartree-Fock correction [19]. This is handled by decomposing the Coulomb kernel into a short-range and a long-range term [21], according to:

$$\frac{1}{r} = \frac{erfc(wr)}{r} + \frac{erf(wr)}{r}, \quad (2)$$

in which erf and erfc are, respectively, the error and the complementary error function. Choosing $w = 0.3$ Å^{-1} leads to the HSE03 functional, whereas $w = 0.2$ Å^{-1} leads to the HSE06 functional [20,22].

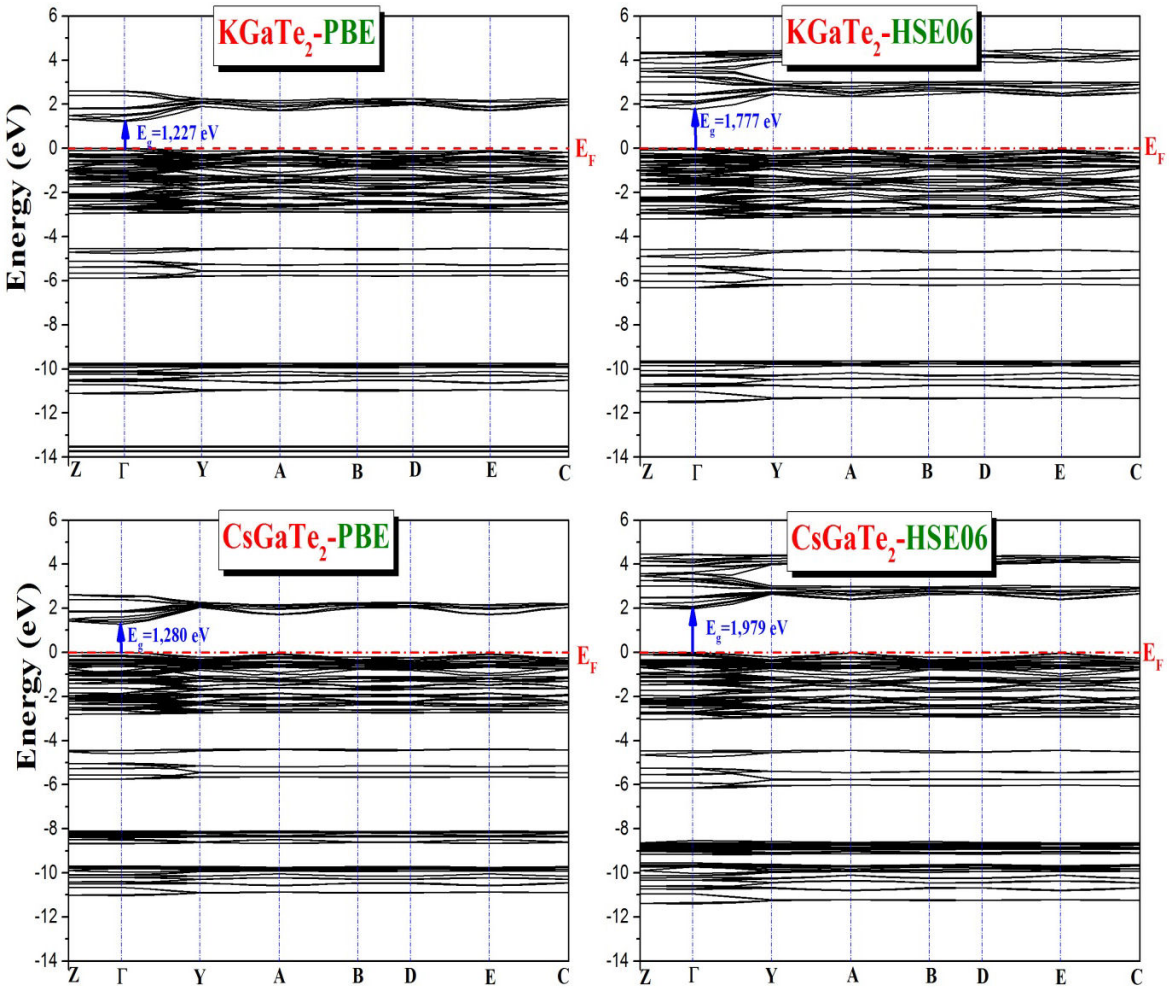

FIGURE 3. Band structure of $KGaTe_2$ and $CsGaTe_2$ calculated along high symmetry lines.

TABLE IV. Calculated refractive index (n), high frequency dielectric constant ϵ_∞, reflection coefficient R for $KGaQ_2$ (Q=S, Se) and $AGaTe_2$ (A=K, Cs).

System	$KGaS_2$	$KGaSe_2$	$KGaTe_2$	$CsGaTe_2$
n	[a]2.313	[a]2.458	[a]2.704	[a]2.632
	[b]2.025	[b]2.470	[b]2.982	[b]2.857
	[c]2.238	[c]2.452	[c]2.778	[c]2.689
ε_∞	[a]5.348	[a]6.040	[a]7.312	[a]6.928
	[b]4.101	[b]6.099	[b]8.894	[b]8.163
	[c]5.011	[c]6.013	[c]7.718	[c]7.229
R	[a]0.157	[a]0.178	[a]0.212	[a]0.202
	[b]0.115	[b]0.179	[b]0.248	[b]0.232
	[c]0.146	[c]0.177	[c]0.222	[c]0.210

a : Ravindra model b : Moss model c :Heve and Vanadamme model

In general, the GGA-PBE functional method does not produce the exact value for the band gap; it underestimates the band gap value [25] while the nonlocal hybrid functional method developed by Heyd, Scuseria, and Enzerhof (HSE06) gives better estimation of electronic properties of solids. This method yields a band gap comparable with the experimental one by including the exact contribution of the Hartree-Fock exchange [21-24,26], the HSE06 functional hybrid density replaces the slowly decomposing long-range part of the exchange Fock by the density functional counterpart. For this reason, to better estimate the electronic bandgap value, we have also used HSE06 in addition of GGA-PBE for comparison.

The band structures calculated along the high symmetry directions: $Z(0,0,1/2)$, $\Gamma(0,0,0)$, $Y(0,1/2,0)$, $A(^1/2,1/2,0)$, $B(1/2,0,0)$, $D(1/2,0,1/2)$, $E(1/2,1/2,1/2)$, $C(0,1/2,1/2)$, $F(0,1/2,0)$ and $Q(0,1/2,1/2)$ in the irreducible Brillouin zone, using the pseudo-potential plane wave (PP-PW) method with the two approaches GGA-PBE and HSE06 for the four materials $KGaS_2$, $KGaSe_2$, $KGaTe_2$ and $CsGaTe_2$, at their equilibrium structural parameters, are plotted in Figs. 2, 3. The estimated band gap values using both GGA-PBE and HSE06 approximations are summarized in Table III with experimental and theoretical data available in the literature for comparison.

The obtained band diagrams have the same form, since the conduction band minima and valence band maxima of all studied materials appear at the center of the Brillouin zone, the Γ point, indicating that all the studied compounds are direct band gap semiconductors according to the calculations by either GGA-PBE or HSE06. We notice also that the HSE06 functional gives notably larger band gaps than the GGA-PBE functional. There is a notable difference between the band gap values yielded by these two functionals. The difference is 0.73 eV, 0.82 eV, 0.55 eV and 0.70 eV for $KGaS_2$, $KGaSe_2$, $KGaTe_2$ and $CsGaTe_2$ respectively. From the Table III, it is clear that the GGA-PBE functional method underestimates the electronic bandgap in the case of $KGaSe_2$ while HSE06 functional method is in better agreement with the experimental value. There are no reported experimental or theoretical results on the band gaps for the remaining compounds, so this is their first theoretical prediction.

On the other hand, it can be observed that the fundamental band gap reveals a decreasing trend on increasing size of chalcogen from S, Se to Te in the case of $KGaQ_2$ (Q=S, Se, Te). The larger band gap is observed in the case of $KGaS_2$, we explain that S is more electronegative than Se and Te, this is consistent with the conclusions of the previously reported study which indicate that the band-gap is inversely proportional to the cell volume [26].

It can be seen that, in GGA-PBE calculations, the band gap value was equal to 2.588 eV and 1.781 eV for $KGaS_2$ and $KGaSe_2$ respectively. The gap energy value in the case of $KGaSe_2$ compound is much smaller than the experimental value [2]. However, the use of the HSE06 hybrid functional gives 3.321 eV and 2.604 eV for $KGaS_2$ and $KGaSe_2$ respectively. We notice that the calculated band gap value by HSE06 is basically consistent with the experimental value in th case of $KGaSe_2$. We have also calculated the band gap of $AGaTe_2$ (A=K, Cs), finding that the values increase by the use of HSE06, from 1.227 eV ($KGaTe_2$) and 1.280 eV ($CsGaTe_2$) to 1.777 eV and 1.979 eV respectively. However, by changing from S, Se to Te in $KGaQ_2$ (Q=S, Se, Te) an important difference is noticed in gap energy value almost of 1 eV and on the other hand the replacement of K-atom by Cs-atom in $AGaTe_2$ (A=K, Cs) induces only a small difference of almost 0.2 eV. There are no reported experimental or theoretical results on the band gaps for $AGaTe_2$ (A=K, Cs), so this is their first theoretical prediction. However, the hybrid density functional theory has improved the band gap, where we find larger band gap values than those obtained by GGA-PBE functional. According to the literature, as mentionned before, GGA-PBE calculations underestimate the band gaps

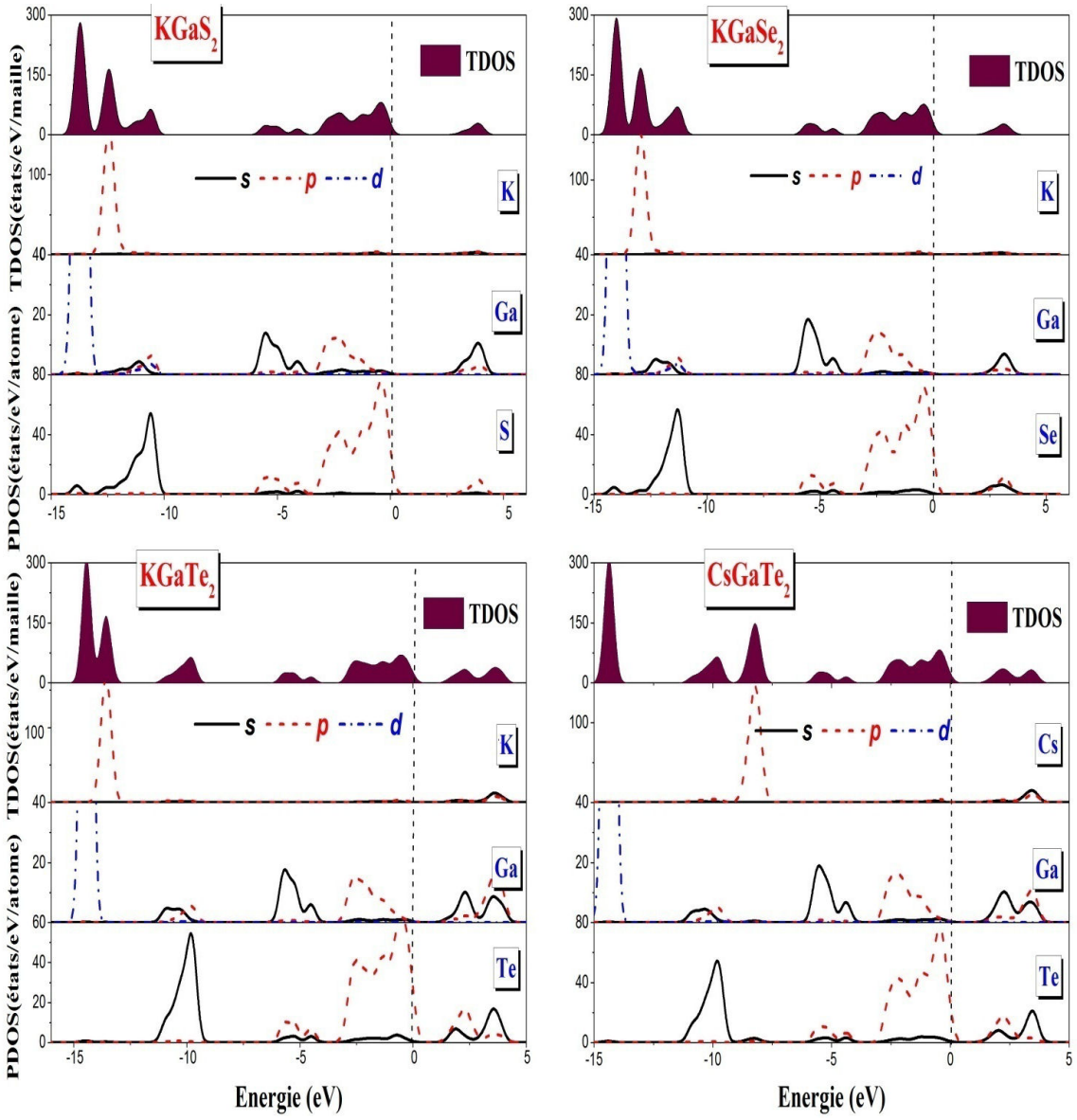

FIGURE 4. Calculated total (TDOS) and partial density of states (PDOS) of $KGaQ_2$ (Q=S, Se, Te) and $CsGaTe_2$.

and HSE06 calculations gives better estimation of band gaps, therefore the obtained gap value using the HSE06 confirms that the studied compounds are direct band-gap semiconductors with wide band-gaps.

Figure 4 represents the total and partial densities of states (TDOS and PDOS) of $KGaQ_2$ (Q=S,Se) and $AGaTe_2$ (A=K, Cs) compounds using the HSE06 approximation. Fermi level is set as zero energy. The valence states are regrouped in three divisions. First, we notice that at lower energies (<-15 eV) there are bands centered on -28.9 eV (-29.4 eV, -30 eV) for $KGaS_2$ ($KGaSe_2$, $KGaTe_2$) respectively and on -21.45 eV for $CsGaTe_2$, formed only of K-s and Cs-s states, which are not shown in the figure for clarity purpose, they do not form chemical bonding to other. And, the bands centered around -13.7 eV for $KGaS_2$, -14 eV for $KGaSe_2$ and -14.4eV for $KGaTe_2$ ($CsGaTe_2$) are mainly formed of gallium Ga-d states. Next, the K-p states are located at -12.5 eV, -12.9 eV, -13.6 eV for $KGaQ_2$ (Q=S, Se, Te) and the Cs-p states at -8.2eV for $CsGaTe_2$. As well as the chalcogen-s states are located at -10.6 eV and -11.3 eV for $KGaS_2$ and $KGaSe_2$ successively and at -9.8 eV for $KGaTe_2$ ($CsGaTe_2$). The K-p (Cs-p) and the chalcogen-s states exhibit very low hybridization, indicating weak chemical bonding between the K (Cs) atom and the chalcogen atoms. Finally, the upper valence band ranging from about -3.3 eV to 0 eV is mainly formed by the chalcogen-s,p and small contribution from Ga-s,p states. We notice a fairly large mixture of the Ga states and the chalcogen states for the title materials, and no contribution of potassium or cesium states around the Fermi level in this region, indicating that the band gap is primarily determined by the $[GaQ2]^-$ layer (Q=S, Se, Te).

The conduction band is formed by chalcogen -s,p states with a small contribution of the Ga-s,p and K(Cs)-s,p states. For all studied compounds, we note that the contribution of potassium states is negligible. Our results of the DOS spectra are approximately similar with those reported in literature [2].

In summary, and as we have seen above, Table III shows the band-gap values of the $KGaQ_2$ (Q=S,Se,Te) and $CsGaTe_2$ materials, where the band-gap value 3.321 eV for $KGaS_2$ is the largest among the four, followed by 2.604 eV for $KGaSe_2$ and 1.777 eV for $KGaTe_2$, and increases to 1.979 eV for $CsGaTe_2$ when replacing the potassium atom by cesium atom. This is agreeing with the previously reported results, which indicate that the value of the band gap is inversely proportional to the cell volume [26]. The anionic radius increasing (1.84 Å, 1.98 Å, 2.21 Å for S, Se and Te successively) increases the cell volume (Table I) leading to a decrease in the minimum conduction band which causes the observed decrease in the band gap. Thus, the existence of direct and wide bandgaps of the studied materials indicates their their possible photovoltaic applications.

3.3. Optical properties

Energy gap and refractive index are two important physical parameters that characterize the electronic and optical properties of semiconductors. Since the energy gap determines the photon absorption threshold in semiconductor and the refractive index is a measure of it transparency with respect to incident spectral radiation, they are useful for determining the suitable applications of semiconductor in electronic, optical and optoelectronic devices.

In the literature, several studies on known semiconductors have been carried out to understand the correlation between the energy gap and the refractive index in order to generate the relation between them. Different empirical models have been proposed, among the best known which have been applied successfully to direct band gap semiconductors are the model proposed by Ravindra in 1979 [13] and that proposed by Moss in 1985 [14]. It was seen that where Ravindra's relation fails Moss's relation approaches experimental results. On the other hand, in 1995, Heve and Vandamm claimed that their model is accurate for wide band gap semiconductors and for most materials used in optoelectronic devices [15].

In this work, the refractive index n was estimated using the three different empirical models, cited above, based on the previously calculated fundamental energy gap E_g, estimated from the HSE06 approximation, using the following equations:

- Ravindra relation [13]:

$$n = \alpha + \beta E_g, \tag{3}$$

with $\alpha = 4.084$ and $\beta = -0.62$ eV^{-}.

- Moss relation [14]:

$$n^4 E_g = k, \tag{4}$$

where k is a constant with a value of 95 eV.

- Herve-Vandamme relation [15]:

$$n = \sqrt{1 + \left(\frac{A}{E_g + B}\right)^2}, \tag{5}$$

with $A = 13.6$ eV and $B = 3.4$ eV. The high-frequency dielectric constant ϵ_∞ can be calculated using the relation

$$\epsilon_\infty = n^2. \tag{6}$$

The reflection coefficient R for high frequencies is given by the relation

$$R = \frac{(n-1)^2}{(n+1)^2}. \tag{7}$$

We have calculated the reflection coefficient R and the high-frequency dielectric constant ϵ_∞ of the studied materials using Eqs. (6) and (7) as function of the refractive index n. The results are presented in Table IV. It can be observed, and whatever the empirical model used, that the refractive index decreases with increasing the energy gap. It is clear that both values of n and ϵ_∞ increase from $KGaS_2$ to $KGaSe_2$ then to $KGaTe_2$ and also decrease from $KGaTe_2$ to $CsGaTe_2$. It can be concluded that the smaller the energy band gap, the higher the refractive index and dielectric constant and the smaller the reflection coefficient, the more useful the material to optoelectronic devices.

We recall that the results presented in the actual paper on n and ϵ_∞ are not available from experimental data or other theoretical studies for comparison, and this results remain as predictions. Moreover, we can remark that the obtained results show that the Herve and Vandamme model represents, generally, the average values between the results using Moss and that of Ravindra. According to the literature, Heve and Vandamme based their equation on oscillatory theory, assuming the UV resonance energy has a constant difference with the band energy. However, they found that their model produces results very close to the experimental data for energy gaps greater than 1.43 eV [27]. Therefore, we believe that the results that could be considered a good prediction are those obtained by the use of the model proposed by Herve and Vandamme.

4. Conclusion

In conclusion, we have studied the structural, electronic and optical properties of $KGaQ_2$ (Q=S, Se) and $AGaTe_2$ (A=K, Cs), using the first principles density functional calculations. The calculated structural parameters of these compounds agree well with the reported experimental data. We have

calculated and compared the electronic structure using both GGA-PBE and HSE06 functionals. Our results show that the four studied compounds are direct band-gap semiconductors with wide band-gaps. We have also estimated the refractive index, the re ection coefficient and the dielectric constant on high frequencies. We expect these materials to have important applications in optoelectronics. Since no known experimental data have been published, we hope that the results presented in this paper will contribute to the literature and generate further theoretical and experimental research.

1. J. Kim and T. Hughbanks Synthesis and structures of ternary chalcogenides of aluminum and gallium with stacking faults: KMQ2 (M=Al,Ga; Q=Se,Te), *Journal of Solid State Chemistry* **149** (2000) 242. https://doi.org/10.1006/jssc.1999.8523.
2. K. Feng, D. Mei, L. Bai, Z. Lin, J. Yao and Y. Wu Synthesis, structure, physical properties and electronic structure of KGaSe2, *Solid state sciences* **14** (2012) 1152. https://doi.org/10.1016/j.solidstatesciences.2012.05.028.
3. J. Weis, H. Schäfer and G. Schön, New ternary element (I)/element (III)-tellurides and selenides, *Z. Naturforsch. B*, **31** (1976) 1336. https://doi.org/10.1515/znb-1976-1008.
4. P. Lemoine, D. Carré and M. Guittard, Structure du sulfure de gallium et de potassium KGaS2, *Acta Crystallographica Section C: Crystal Structure Communications* **40** (1984) 910. https://doi.org/10.1107/S0108270184006223.
5. E. Wu, M. Pell, T. Fuelberth, and J. Ibers, Crystal structure of caesium gallium ditelluride, CsGaTe2, *Zeitschrift fü Kristallographie-New Crystal Structures* **212** (1997) 91. https://doi.org/10.1524/ncrs.1997.212.jg.91.
6. D. Friedrich, M. Schlosser, M. Etter, and A. Pfitzner, Influence of Alkali Metal Substitution on the Phase Transition Behavior of $CsGaQ_2$ (Q= S, Se), *Crystals* **7** (2017) 379. https://doi.org/10.3390/cryst7120379.
7. S. Clark *et al*., First principles methods using CASTEP, *Zeitschrift fü Kristallographie-Crystalline Materials* **220** (2005) 567. https://doi.org/10.1524/zkri.220.5.567.65075.
8. J. P. Perdew, K. Burke, and M. Ernzerhof, Generalized gradient approximation made simple, *Physical review letters* **77** (1996) 3865, https://doi.org/10.1103/PhysRevLett.77.3865.
9. D. Vanderbilt, Soft self-consistent pseudopotentials in a generalized eigenvalue formalism, *Physical review B* **41** (1990) 7892, [Erratum *Phys. Rev. Lett*. **78** (1997) 1396], https://doi.org/10.1103/PhysRevB.41.7892.
10. T. H. Fischer and J. Almlof, General methods for geometry and wave function optimization, *The Journal of Physical Chemistry* **96** (1992) 9768. https://doi.org/10.1021/j100203a036.
11. H. J. Monkhorst and J. D. Pack, Special points for Brillouin-zone integrations, *Phys. Rev. B* **13** (1976) 5188. https://doi.org/10.1103/PhysRevB.13.5188.
12. A. V. Krukau, O. A. Vydrov, A. F. Izmaylov, and G. E. Scuseria, Influence of the exchange screening parameter on the performance of screened hybrid functionals, *J. Chem. Phys.* **125** (2006) 224106, https://doi.org/10.1063/1.2404663.
13. N. M. Ravindra, S. Auluck, V. K. Srivastava, On the Penn gap in semiconductors, *Physica status solidi (b)* **93** (1979) K155, https://doi.org/10.1002/pssb.2220930257.
14. T. S. Moss, Relations between the refractive index and energy gap of semiconductors, *physica status solidi (b)* **131** (1985) 415. https://doi.org/10.1002/pssb.2221310202.
15. P. J. L. Hervè and L. K. J. Vandamme, Empirical temperature dependence of the refractive index of semiconductors, *Journal of Applied Physics* **77** (1995) 5476. https://doi.org/10.1063/1.359248.
16. A. Alkauskas, P. Broqvist and A. Pasquarello, Defect levels through hybrid density functionals: Insights and applications, *Physica status solidi (b)* **248** (2011) 775. https://doi.org/10.1002/pssb.201046195.
17. S. Kümel, and L. Kronik, Orbital-dependent density functionals: Theory and applications, *Rev. Mod. Phys.* **80** (2008) 3. https://doi.org/10.1103/RevModPhys.80.3.
18. A. D. Becke, A new mixing of Hartree Fock and local density functional theories, *J. Chem. Phys.* **98** (1993) 1372. https://doi.org/10.1063/1.464304.
19. C. Mietze *et al.*, Band offsets in cubic GaN/AlN superlattices, *Phys. Rev. B* **83** (2011) 195301. https://doi.org/10.1103/PhysRevB.83.195301.
20. J. Heyd, G. E. Scuseria and M. Ernzerhof, Hybrid functionals based on a screened Coulomb potential, *J. Chem. Phys.* **118** (2003) 8207. https://doi.org/10.1063/1.1564060.
21. M. Landmann *et al*., Transition energies and direct-indirect band gap crossing in zinc-blende AlxGa1-xN, *Phys. Rev. B* **87** (2013) 195210. https://doi.org/10.1103/PhysRevB.87.195210.
22. J. Heyd, J. E. Peralta G. E. Scuseria and R. L. Martin, Energy band gaps and lattice parameters evaluated with the Heyd-Scuseria-Ernzerhof screened hybrid functional, *J. Chem. Phys.* **123** (2005) 174101. https://doi.org/10.1063/1.2085170.
23. J. Paier *et al*., Screened hybrid density functionals applied to solids, *J. Chem. Phys.* **124** (2006) 154709. https://doi.org/10.1063/1.2187006.
24. M. Marsman, J. Paier, A. Stroppa and G. Kresse, Hybrid functionals applied to extended systems, *Journal of Physics: Condensed Matter* **20** (2008) 064201. https://doi.org/10.1088/0953-8984/20/6/064201.

25. V. L. Shaposhnikov, A. V. Krivosheeva, V. E. Borisenko, J.-L. Lazzari, and F. Arnaud, d'Avitaya, Ab initio modeling of the structural, electronic, and optical properties of A II B IV C 2 V semiconductors, *Phys. Rev. B* **85** (2012) 205201. https://doi.org/10.1103/PhysRevB.85.205201.

26. L. Tang, M. Lee, C. Yang, J. Y. Huang, and C. Chang, Cation substitution effects on structural, electronic and optical properties of nonlinear optical AgGa(SxSe1-x)2 crystals, *Journal of Physics: Condensed Matter* **15** (2003) 6043. https://doi.org/10.1088/0953-8984/15/35/312.

27. N. M. Ravindra, P. Ganapathy and J. Choi, Energy gap refractive index relations in semiconductors-An overview, *Infrared physics and technology* **50** (2007) 21. https://doi.org/10.1016/j.infrared.2006.04.001.